Neuroscience and Geographic Information Systems to Investigate the Impact of Global Warming on Mood Disorders and Brain Plasticity in Urban Areas

Marco Vieira Ruas, Romana Paganini, Bogdan Draganski, and Stéphane Joost

Abstract Geographic Information Systems (GIS) are advanced computational systems for acquiring, storing, analyzing, and visualizing spatial data, enabling comprehensive exploration of geographical relationships and patterns across diverse domains. GIS play a crucial role in analyzing the intersection of mood and brain data in a geo-environmental context. Through spatial analysis techniques, GIS

M. Vieira Ruas
Geospatial Molecular Epidemiology group (GEOME), Laboratory for Biological Geochemistry (LGB), Ecole Polytechnique Fédérale de Lausanne (EPFL), Lausanne, Switzerland

Geographic Information Research and Analysis in Population Health (GIRAPH), Geneva University Hospitals, Geneva, Switzerland

R. Paganini
Section of Environmental Science and Engineering (SIE), Ecole Polytechnique Fédérale de Lausanne (EPFL), Lausanne, Switzerland

B. Draganski
Laboratory for Research in Neuroimaging, Department of Clinical Neurosciences, Lausanne University Hospital and University of Lausanne, Lausanne, Switzerland

Neurocentre, Neurology Department, Inselspital - University Hospital Bern, Bern, Switzerland

S. Joost (✉)
Geospatial Molecular Epidemiology group (GEOME), Laboratory for Biological Geochemistry (LGB), Ecole Polytechnique Fédérale de Lausanne (EPFL), Lausanne, Switzerland

Geographic Information Research and Analysis in Population Health (GIRAPH), Geneva University Hospitals, Geneva, Switzerland

Unit of Population Epidemiology, Division of Primary Care Medicine, Geneva University Hospitals, Geneva, Switzerland

La Source School of Nursing, University of Applied Sciences and Arts Western Switzerland (HES-SO), Lausanne, Switzerland
e-mail: stephane.joost@epfl.ch

S. Kühn (ed.), *Environmental Neuroscience*,
https://doi.org/10.1007/978-3-031-64699-7_18

allows researchers to visualize and understand the geographical distribution of mood-related phenomena and their correlation with brain activity patterns.

In this chapter, we show that GIS can offer a powerful framework integrating spatial perspectives for examining the intricate interplay between mood, brain data, and global warming. This interdisciplinary approach enhances our understanding of the psychological impacts of environmental shifts, aiding in the development of targeted interventions to mitigate the mental health consequences of global warming.

On the example of mood disorders, we exemplarily demonstrate how GIS can be implemented to investigate the effects of climate warming on mental health and brain plasticity. We used satellite images to calculate land surface temperature (LST) and LST changes over time in the urban context of the city of Lausanne, Switzerland. These data were compared to mental health and magnetic resonance imaging (MRI) information from a population study in Lausanne.

The distribution of mood disorders exhibited a discernible spatial pattern across Lausanne, indicating that they were not randomly distributed in the geographical space. Spatial clusters with significantly higher rates of mood disorders were associated with significantly higher LST. Conversely, areas with lower LST at residential locations showed significantly better mental health performance.

Keywords Geographic Information Systems (GIS) · Spatial statistics · Spatial dependence · Magnetic Resonance Imaging (MRI) · Urban environment · Climate change · Heat island · Brain plasticity

Introduction

Geographic Information and Neuroscience

In recent years, there has been a growing interest in leveraging GIScience (Goodchild, 1992) and geospatial data to inform public health. The genesis of Geographical Information Systems (GIS) traces back to the 1960s, when the integration of spatial data with computer technology marked a shift in the way geographic information was visualized and analyzed (Chrisman, 2020). This approach has since evolved to integrate hardware, software, and data facilitating a wide range of applications such as environmental conservation (Caniani et al., 2016), urban planning (Zoungrana et al., 2024), agriculture sustainability (Mathenge et al., 2022), and public health surveillance (Di Lorenzo et al., 2023). The utility of GIS extends beyond data visualization; it serves as a powerful analytical tool capable of revealing and examining spatial patterns and relationships (Longley, 2005) that inform decision and policy-making processes (Pedro et al., 2019). In urban settings, an escalating interest has emerged in exploiting georeferenced measurements to study the intricate relationship between social and environmental determinants—i.e., the exposome, brain, and behavioral outcomes. Indeed, the integration of spatial

information with brain data has the potential to reveal important insights into neurological disorders and enhances our understanding of how spatial contexts influence brain health. This interdisciplinary approach, sometimes referred to as neuro-geography (Pykett, 2018), seeks to understand how geographic factors influence brain health and cognitive function (Colantonio et al., 2011; León and Burga-León, 2015). Researchers use a variety of geospatial data sources, such as land use, air quality, proximity to green spaces, and socioeconomic factors, to assess their impact on brain health (Park et al., 2021). For example, studies have explored how exposure to urban green spaces can positively affect mental well-being (Jabbar et al. 2022), or how air pollution may be linked to cognitive decline (Delgado-Saborit et al., 2021). GIS tools are employed to map and visualize the spatial distribution of these environmental variables, allowing researchers to correlate them with neuroimaging data and cognitive assessments (Kühn et al. 2017). The integration of GIScience and geodata provides valuable insights into the complex interplay between the brain and the natural or built environment, shedding light on potential risk factors and strategies for promoting well-being and cognitive health. This field holds promise for enhancing our understanding of the brain-behavior-environment relationships and ultimately improving public health initiatives and urban planning strategies. In the current context of climate change, the ability of GIS to integrate brain data and the characteristics of the urban environment is particularly interesting, and this ability can be used to analyze the possible impact of global warming on human health through effects on brain anatomy.

Climate Change and Mental Health

The effects of climate change are multifaceted and manifest in various aspects of our lives. The impact of global warming and the resulting consequences on human health was investigated in various studies. It is likely to affect not only physical but also mental health (Padhy et al., 2015). Previous research has shown evidence connecting mental disorders, specifically anxiety, with extreme weather events (Palinkas & Wong, 2020). However, merely contemplating climate change and its potential consequences in the future can also contribute to mental distress (Palinkas & Wong, 2020).

The trend of rising land surface temperature (LST) has resulted in more prolonged and intense heatwaves. In urban areas, the air temperature is consistently higher compared to rural areas, a disparity that becomes especially pronounced during the summer months due to the heat island effect. During nighttime, urban areas can show temperatures that are 5–7 °C higher than natural surroundings (Wicki et al. 2018; MeteoSwiss, 2023). This poses a significant risk to human well-being (Berry et al., 2010) and health (Hondula et al., 2015). A well-established association was observed between heatwaves and mental disorders (Thompson et al., 2018), and Obradovich et al. (2018) showed that a temperature increase of 1 °C over 5 years was linked to a 2% rise in mental health problems.

A less explored research area is the potential effect of rising temperatures on brain structures. As a result, the extent to which heat islands affect brain structures is not yet understood and it remains difficult to clearly identify the influence of global warming on neurological disorders (Amiri et al., 2021). Still, the evidence available to date indicates that climate change will have a significant impact on the prevalence and management of major neurological diseases in the near future (Louis et al., 2023).

In this chapter, we exemplarily use georeferenced information (place of residence), GIS and spatial statistics to demonstrate how one can investigate relationships between land surface temperature, mental health, and brain plasticity. We focus on population-based data collected in Lausanne, western Switzerland (Firmann et al., 2008; Preisig et al., 2009). The aims of this study are to examine the impact of increased LST on mood disorders, as well as on brain white matter structure characteristics as recorded using magnetic resonance imaging (MRI). We hypothesized that high LST values are associated with low mental health and high anxiety and that relationships exist between global warming—as translated by higher land surface temperature—mood disorders and characteristics of white matter microstructure.

Data

Geographic Information Systems Data

GIS data have distinct characteristics that enable their inclusion in mapping and in spatial data analyses frameworks. It consists primarily in vector and raster data (Fig. 1), two distinct types corresponding to two different ways of storing digital geographic information.

Vector data are represented through points, lines, and polygons, enabling precise delineation of discrete geographical entities. Points mark specific locations, lines embody linear features such as rivers or roads, and polygons outline areas like countries, lakes, or park boundaries. This data format is complemented by the integration of attribute tables. The latter store information about the features represented in vector data, effectively linking non-spatial data to spatial features. Each row in an attribute table corresponds to a specific spatial feature, while each column represents a distinct attribute of that feature, such as name, type, population, or any other descriptive property.

Raster data, on the other hand, consist of a matrix of cells or pixels, with each cell holding a value representing information such as temperature, elevation, or vegetation density. This data type is ideal for modeling continuous spatial phenomena and is characterized by its resolution, determining the level of detail that can be represented. The resolution is defined by the size each pixel represents on the ground. A finer resolution, characterized by smaller pixels, results in a larger

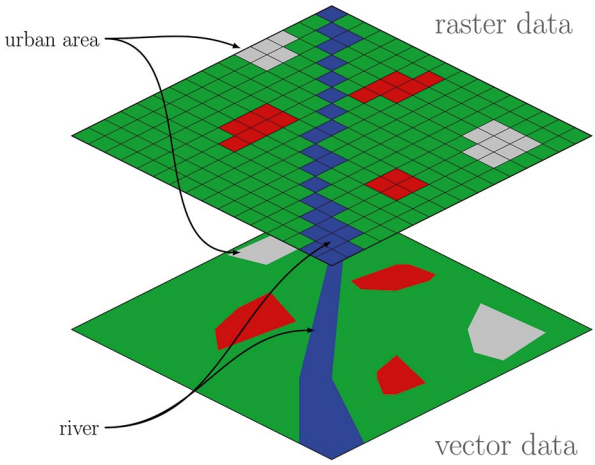

Fig. 1 Representation of superimposed vector and raster data types. (Wegmann, CC BY-SA 3.0, via Wikimedia Commons)

density of values over a given area, thereby enhancing the precision of the data measure and representation.

Vector and raster data are integral to GIS, each serving specific analytical needs. The utilization of both data types relies on the usage of precise coordinates (longitude and latitude) that align the spatial data with a recognized reference system. This alignment allows the accurate mapping and analysis of the data in correspondence with the real world.

In the following data analysis example, the study area is depicted using polygon type data, while the health data are captured within attribute tables linked to the participants' addresses, which are represented as points. Lastly, the LST measurements are presented as a raster grid.

Study Area

The study area consists of the urban area of the city of Lausanne, Switzerland (150,000 inhabitants in 2023). Lausanne is located on the northern shore of Lake Geneva. It is the capital of the canton of Vaud and the administrative center of the Lausanne district. It is the country's fourth-largest city in Switzerland in terms of population, after Zurich, Geneva, and Basel.

Health Data

We utilized health data from the CoLaus-PsyColaus cohort, a longitudinal study in the community dwelling population of Lausanne, Switzerland, initiated in 2003 with 5-yearly follow-ups. At baseline, the cohort involved over 6700 individuals

aged 35–75 years old (Firmann et al., 2008; Preisig et al., 2009). The complete list of Lausanne residents aged 35 to 75 years was provided by the city's population register, and a simple, nonstratified random sample of 35% of this population was drawn. The 8121 people who agreed to participate represented 41% of the population initially sampled. The baseline CoLaus-PsyColaus study recruited 6733 participants (3544 women), of whom 5064 agreed to be recontacted for follow-ups (FU1: 2009–2012; FU2: 2014–2017; FU3: 2018–2021). At baseline and subsequent follow-ups, participants made a single visit to the Lausanne University Hospital (CHUV), which included an interview and physical examination. The mood data used in the present analysis were collected during the second follow-up. In addition, MRI was used to acquire brain structure data from subjects during follow-ups two and three. For each subject, we selected a single scan—their earliest one completed during these periods.

Mood Data

For assessment of anxiety levels, we used Spielberger's et al. (1983; Julian, 2011) State Trait Anxiety Inventory (STAI), divided into STAI state and STAI trait subscores. For each of the subsets, the items' scores were summed to obtain a final score ranging between 20 and 80, with higher values corresponding to higher levels of anxiety. We focused on STAI state, which provides an indication of an individual's current anxiety. For the affective components of social, occupational, and psychological well-being we used the Global Assessment of Functioning (GAF) assessing lifetime (GAF-L), worst (GAF-W), and current (GAF-C) affective state (Bell, 1994). Higher GAF scores range from 1 to 100. Higher scores translate into a better overall well-being.

STAI state and GAF scores were adjusted for age, gender, and neighborhood median income (i.e., median revenue of the neighborhood of the place of the subject's residence in 2017) (MicroGIS, 2017).

Brain Data

We analyzed the brain's white matter (WM) microstructure. Specifically, we investigated 31 tracts of interest identified on the basis of four MRI-derived maps in the context of a previous study that investigated the relationship between WM and cardiovascular risk factors (Trofimova et al., 2023). The four maps correspond to measurements of myelin content (MTsat), axonal density (ICVF), free water (ISOVF), and tract volume (number of voxels) (➔ chapter "Mapping the Human Brain with Computational Anatomy" by Draganski, Joost and Kherif). The methodology and analytical procedures used in the present work are based on the approach described in the aforementioned study (Trofimova et al., 2023). The values of the maps for each tract were adjusted for age, gender and total intracranial volume (TIV). For

each map and tract, only values within the 3-sigma interval around the mean value were included in the analysis to remove errors in the data.

Environmental Data

We used two distinct types of land surface temperature (LST) measurements to assess its relationship with mood and white matter microstructure. These measurements characterize the place of residence of the participants. First, we computed the LST for the follow-up assessment examination year, and second, the LST delta between two periods: period one—between 2004 and 2012—represents the timeframe before follow-up two; and period two—between 2014 and 2021—including follow-ups two and three.

For each year analyzed, LST was calculated using values from June, July, and August, since these months are typically when the heat island effect[1] is most likely to occur in urban areas.

Land Surface Temperature (LST) Calculation

LST measurements were calculated using Landsat satellite imagery (https://landsat.gsfc.nasa.gov/) from the United States Geological Survey (USGS). We employed the Google Earth Engine platform (GEE; https://earthengine.google.com/) for efficient processing and analysis of the satellite imagery. We used Landsat 5 imagery for the years preceding 2012, and Landsat 8 for the subsequent years. The GEE platform was used to derive the LST data from the satellite images using the Statistical Mono-Window algorithm developed by Ermida et al. (2020). To generate the LST data for each year, we collected all relevant images captured during the defined timeframe and for the months of June, July, and August. On average, there were 14 usable images per year. On the basis of these images, we created a single composite image for each summer by calculating the median value for each pixel across all captures within that year. The use of the median value is robust to outliers, such as those caused by cloud cover. This resulting composite image provided a representative depiction of the average LST during the summer for each year, which was crucial for analyzing the variables of interest in conjunction with the actual LST values of the examination year. In a second step, the median images obtained for each year were further aggregated by calculating the mean value over several

[1] We refer here to the definition of heat island as proposed by the United States Environmental Protection Agency (EPA): "Heat islands are urbanized areas that experience higher temperatures than outlying areas. Structures such as buildings, roads, and other infrastructure absorb and re-emit the sun's heat more than natural landscapes such as forests and water bodies. Urban areas, where these structures are highly concentrated and greenery is limited, become "islands" of higher temperatures relative to outlying areas".

years. This aggregation process was performed separately for the periods one and two defined above. To obtain the delta LST variable, the mean image derived from period one was subtracted from the mean image of period 2, allowing for the examination of temperature change over time.

Methods

As regards mood data, we initially calculated the spatial dependence of the variables of interest (GAF and STAI) to identify significant geographic clusters of high or low mood values. Then, we conducted variance analysis to determine if significant differences exist in LST variables (year of examination and delta) across the different mood cluster classes identified (see the spatial statistics section hereunder).

For brain white matter data, we first calculated a linear regression between the four MRI-derived maps investigated and LST measurements, for each of the 31 tracts of interest. We only considered significant associations for subsequent spatial examination and variance analysis across the identified clusters.

Georeferencing

We utilized georeferencing, to assign the home addresses provided by participants during the follow-ups to specific longitude and latitude coordinates. To achieve this, we employed the Swiss Confederation GeoAdmin API.[2] In Switzerland, the extensive cataloging and geolocation of every street and road facilitate the precise georeferencing of every building. By submitting an address through an API request, we receive a list of attributes, including the coordinates corresponding to that address.

Assigning Exposome Values to Individuals and Buffer Zones

To assign the calculated LST measurements to each corresponding individual, we leveraged the intersection between the participants' georeferenced addresses, depicted as points, and the corresponding LST raster pixel values. Using a GIS sampling tool, we matched the address points with the LST data contained within the 30 × 30 m pixels of their location. We subsequently stored the extracted values from the raster layers in an appropriate column in the attribute table of the address points.

[2] Coordination and Geo-Information Services (COGIS) of the Swiss Confederation, API REST Services—GeoAdmin API 3.0, https://api3.geo.admin.ch/services/sdiservices.html?#search (accessed 9.14.23).

In this instance, we employed a straightforward geographic intersection between points and raster pixels, aiming to obtain LST values near the home address. However, the broader assessment of the environmental exposome typically involves creating buffer zones around home (or other) addresses. This approach enables the calculation of crow-fly median values at various radii surrounding the subjects' home addresses, providing a more comprehensive evaluation of environmental exposure.

The chosen radius length is dictated by the potential impact range of the environmental exposome factor under study. For instance, certain environmental exposome factors, like nighttime traffic noise, necessitate smaller buffer zones—typically no more than 25–50 m—since their effects diminish rapidly with distance from the source. Conversely, vegetation density assessment may require broader ranges, from 25 m for immediate vicinity considerations to up to 5 km (Dimitrov-Discher et al., 2022) for evaluating access to public parks rather than direct visibility or exposure at the residence. Understanding the spatial extent and lag of the effects is crucial in spatial analysis to measure spatial dependence. Accordingly, methodologies have been refined to mathematically ascertain spatial weight matrices (Yu & Fotheringham, 2022).

Furthermore, the choice of buffer zones for assessing environmental exposome factors, especially in studies focusing on accessibility, may shift from simple crow-fly buffers to those that incorporate the specific street network accessible from a participant's home address. This approach enables the measurement of distances based on the actual time it takes for a subject to traverse the path, allowing for the addition of "costs" to the journey. These costs could account for factors such as slope or road obstructions, which impact the distance subjects can cover within a given time frame.

Spatial Statistics

Spatial dependence denotes the tendency for nearby locations to influence each other within a certain distance and share similar features (Goodchild, 1992). Objects or individuals in proximity tend to be more similar than objects or individuals that are farther apart (Tobler, 1970). This principle holds true when examining disease occurrence across a territory, or the geographical distribution of health indicators. Indeed, individuals who share the same environment are exposed to similar social and environmental determinants. Habits and automatisms are easily shared (Marteau et al., 2012) by mimicry (Duffy et al., 2020) within neighborhoods. Spatial autocorrelation is the statistical measure that quantifies this similarity of attributes between sample point locations—i.e., where individuals live. Additionally, the principle that geographical location significantly influences measured values is recognized as spatial dependence.

Several statistics have been developed to measure spatial autocorrelation. The most used is Moran's I (Moran, 1950), which quantifies globally over a given

territory the similarity between the attributes of all objects or individuals and their N neighbors, or those located within a given radius. Local versions of this statistic are the local Moran's I (Anselin, 1995) or the Getis-Ord Gi* statistics (Getis & Ord, 1992), capable of quantifying and categorizing locally the similarity or dissimilarity between behaviors. Their calculation amounts to a Z score, with the null hypothesis assuming a random spatial pattern for the analyzed values.

We assessed the spatial dependence of the mood measurements and brain anatomy with the Getis-Ord statistics implemented in Python. Statistical significance was tested using 999 permutations with a significance level of 0.05. Statistically significant positive and negative Z scores are represented respectively by hot spots (HS)—clusters of high values, and cold spots (CS)—clusters of low values. Neutral sampling sites are labeled nonsignificant (NS). On the maps produced, hot spots are shown in red, cold spots in blue and nonsignificant in white. Getis-Ord Gi* was calculated using spatial lags of 200 m, 400 m, 600 m, and 800 m (sensitivity analysis). We selected the spatial lag of 600 m to produce the maps shown on Figs. 3a, 4a and 6a. This specific spatial lag highlights interesting spatial patterns while avoiding excessive spatial aggregation.

The application of spatial statistics to precisely georeferenced individual locations is key as this avoids errors that could be caused by a problem called the modifiable areal unit problem (MAUP; Openshaw, 1984). MAUP—a form of ecological fallacy—is a critical issue in spatial analysis, highlighting how the outcomes of such analyses can be significantly influenced by the scale of aggregation and the delineation of spatial units. This problem manifests in two key ways: through the scale effect, where the granularity of data aggregation (e.g., hectometric grid, city, region, and country) can alter analytical results, potentially masking local variations at broader scales, and the zoning effect, where variations in the configuration of spatial unit boundaries can lead to different interpretations of the same underlying data. MAUP's implications emphasize the necessity for carefully justified choices of scale and zoning to ensure accurate spatial analysis outcomes. One of our example study's strengths lies in its use of fine-scale georeferenced measurements and analysis at an individual level, which surpasses the limitations of studies using predefined units.

Variance Analysis

We calculated group averages of LST and delta LST measurements for the spatial clusters obtained from the Getis-Ord calculation. We assessed homogeneity of LST data across clusters with the Levene's test (Levene, 1960). The Levene's test evaluates the null hypothesis according to which the distinct groups of individuals analyzed are of equal variance. For LST data showing homogeneity across clusters, we calculated a one-way ANOVA (Ståhle and Wold, 1989) and the subsequent Tukey post-hoc test (Tukey, 1949) for multiple pairwise comparisons. In cases of

heterogeneous LST measurements, we performed a one-way Kruskal–Wallis (KW) test (Kruskal and Wallis, 1952) and a non-parametric post-hoc Conover test.

In addition, the eta-squared from both the ANOVA and the KW test provides information about the effect size observed. It is the amount of variation explained by the predictor variable. Effect sizes larger than 0.01 indicate a small effect (Coe, 2002). Therefore, any effect size below this threshold is considered negligible.

Linear Regression

We computed ordinary least squares (OLS) linear regression to calculate the associations between the four MRI-derived maps (myelin content, axonal density, free water, and tract volume) and LST of the examination year and LST delta. This analysis was performed for all 31 tracts.

Results

Subjects Included in the Analysis

Only a subset of the total population was selected for our analyses. On the one hand, we focused on the dense urban part of the city, within a perimeter defined by 11 communes (Lausanne, Renens, Paudex, Pully, Belmont-sur-Lausanne, Ecublens, Prilly, Chavannes-près-Renens, Le Mont, Bussigny, and Epalinges). Additionally, a small number of participants were excluded from the analysis due to missing information regarding confounding variables (age, gender, income, and TIV).

As regards WM data, additional participants were excluded when their values fell outside of the three-sigma interval around the mean. These data points were considered to be erroneous data. However, 98.9% of the data were within this interval. We therefore have a different number of individuals for each type of variable. Information on the number of subjects per variable is given in Table 1.

LST and Delta LST

Land surface temperature of the urbanized areas, particularly in the city center of Lausanne and in the western region, exhibits higher values and highlight the urban heat island effect (Fig. 2a). In some places, LST reached up to more than 37 °C. In contrast, the peripheral regions including the northern districts, show substantially lower LST (between 25 and 30 °C). Notably, the shores of the lake and the forest

Table 1 Participant's characteristics for each health variable

	GAF	STAI	Brain
Follow-up	F2	F2	First examination in F2 and F3
Total number of subjects	3647	2470	1582
# of subjects analyzed	2991	2174	1258[a]
% men/women[b]	43.7/56.3	42.8/57.2	47.6/52.4
Mean age (sd) [years][b]	62.9 (10.3)	63.5 (10.1)	63.5 (9.5)

[a]Depending on the tract and map, subjects with outstanding values (outside the 3-sigma interval around the mean) were excluded from the analysis (on average, 98.9% of the values were within the interval)
[b]Referring to the number of subjects analyzed

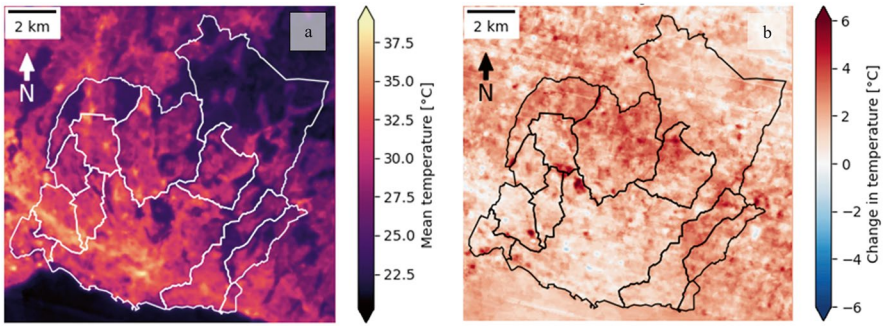

Fig. 2 On the left (**a**), average land surface temperature (LST) calculated for each pixel (30 m × 30 m) between 2014 and 2021 during the months of June, July and August. On the right (**b**), average difference in LST between 2014 and 2021. Delta LST = mean(2014–2021)—mean(2004–2012)

areas, such as the district in the north-east, show the lowest temperatures indicating their cooling effect.

As regards delta LST (Fig. 2b), we can observe a general signal of temperature increase across the area of interest. The magnitude of temperature deltas locally varies, with some areas experiencing even a decrease in dense urban areas (see blue spots). Most pixels show either a slight rise or a more substantial increase of up to 6 °C. Notably, the districts to the north of the urbanized area (center of the image) experience the highest temperature increase.

Mood Variables

Global Assessment of Functioning (GAF)

Variance analysis of LST of the examination year across GAF-Current clusters assessed with spatial lags of 600 m and 800 m showed the most substantial effect sizes. We found that the results across GAF-lifetime and GAF-worst clusters were

negligible. Additionally, our findings show that the variance attributable to delta LST was predominantly significant across GAF-current clusters, although results across GAF-lifetime and to a lesser extent GAF-worst were above the 0.01 threshold. We present in Fig. 3a the spatial distribution of GAF-current clusters with a 600 m spatial lag and the associated LST measurements in boxplots (Figs. 3b and 3c).

We identified a primary GAF-Current coldspot (lower current well-being) in the city center, north of the main train station. Conversely, we found GAF-current hotspots (better current well-being) in the peripheric regions. The boxplots in Figs. 3b and 3c illustrate the distribution of LST measurements at the residences of subjects within hotspots, coldspots and neutral geographic space. Both the LST of the examination year and delta LST demonstrated dose-response effects across clusters, albeit in an inverse relationship: average LST measurements of the examination year were higher in GAF-Current coldspots ($p \leq 0.001$), whilst average delta LST measurements were higher in hotspots. Specifically, hotspots recorded high LST deltas (mean = +1 °C), in contrast to the lower LST deltas in coldspots (mean = +0.3 °C). The effect sizes for the corresponding ANOVA analyses, 0.014 and 0.015, were small but non-negligible.

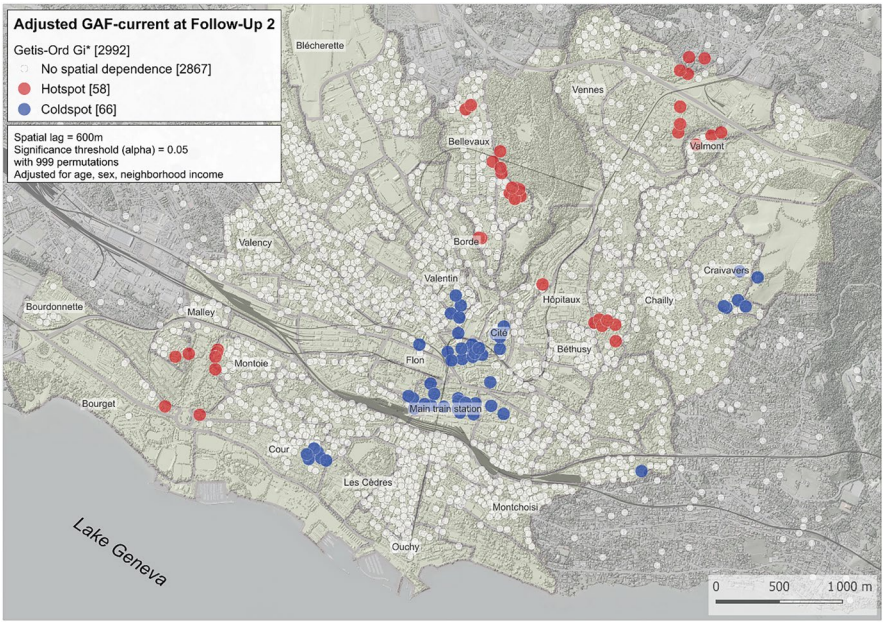

Fig. 3a A dot represents a single subject. Subjects belong either to Global Assessment of Functioning (GAF-Current) hotspots (HS) in red (significant grouping of 58 high GAF-Current values), to GAF-Current coldspots (CS) in blue (significant grouping of 66 low GAF-Current values), or to the neutral geographic space (NS) in white, for a spatial lag of 600 m. GAF-Current was adjusted for age, sex and neighborhood median income. Significance threshold is 0.05 for 999 permutations

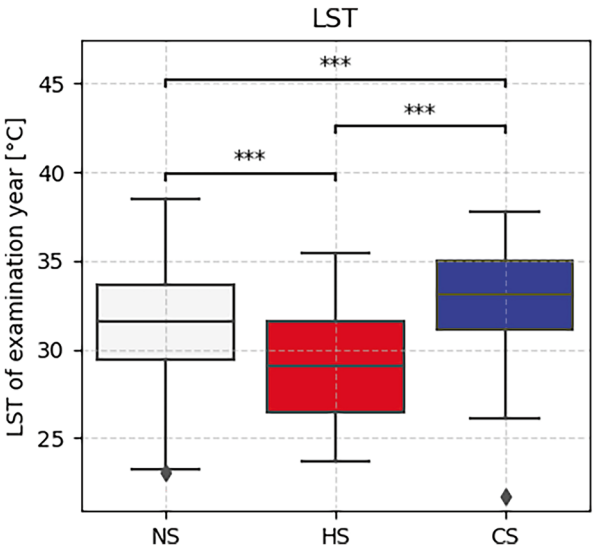

Fig. 3b Boxplots of land surface temperature (LST) values within the three types of Global Assessment of Functioning (GAF-Current) clusters shown on Fig. 3a. Low GAF-Current values show low LST, while high GAF-Current show high LST. GAF-Current values where geography's influence is neutral show intermediate LST values. All pairwise comparisons (Tukey HSD) between Getis-Ord classes are significant. Not significant: $p \geq 0.05$; *: $p \leq 0.05$; **: $p \leq 0.01$; ***: $p \leq 0.001$

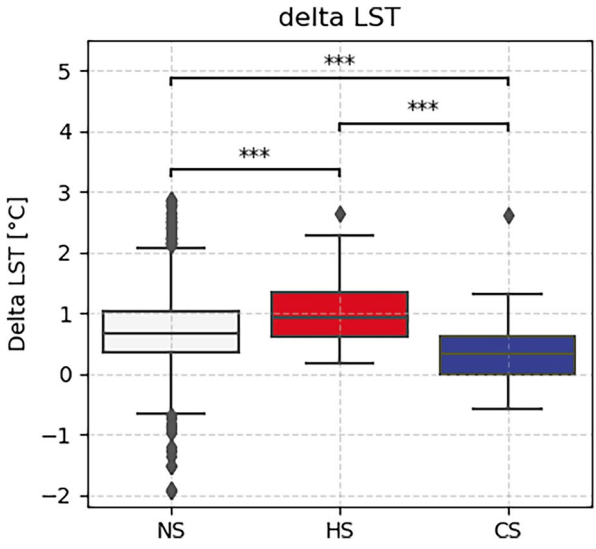

Fig. 3c Boxplots of delta Land Surface Temperature (LST) values within the three types of Global Assessment of Functioning (GAF-Current) clusters shown on Fig. 3a. High GAF-Current values show high delta LST, while low GAF-Current show low delta LST. GAF-Current values where geography's influence is neutral show intermediate delta LST values. All pairwise comparisons (Tukey HSD) between Getis-Ord classes are significant. Not significant: $p \geq 0.05$; *: $p \leq 0.05$; **: $p \leq 0.01$; ***: $p \leq 0.001$

State-Trait Anxiety Inventory (STAI)

Variance analysis revealed that both LST of the examination year and delta LST measurements presented the highest effect size across clusters of STAI state calculated with a 600 m spatial lag. We detected a primary STAI state hotspot (higher anxiety state levels) to the northwest and a secondary one to the east of the city center (Fig. 4a). Moreover, we found a large STAI state coldspot (lower anxiety state levels) in the northern part of the city and smaller ones in the western and southern parts. Subjects residing in the southern city area beneath the railway typically belonged to the non-significant cluster class. LST of the examination year was higher ($p \leq 0.0001$) in anxiety state hotspots (Fig. 4b), whereas delta LST was lower ($p \leq 0.0001$) these hotspots (Fig. 4c). The effect sizes for the corresponding respective KW analyses were 0.028 and 0.021.

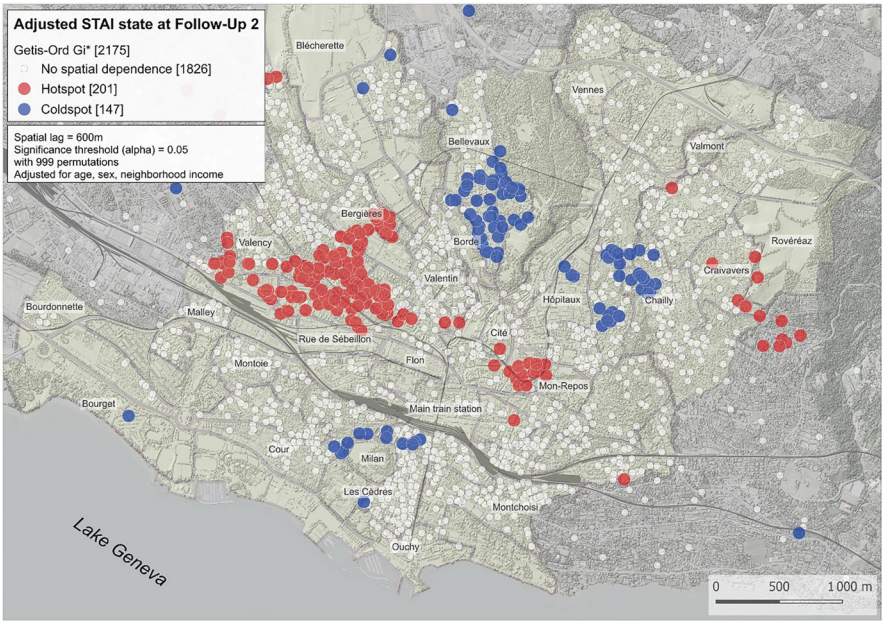

Fig. 4a A dot represents a single subject. Subjects belong either to State Trait Anxiety Inventory (STAI) state hotspots (HS) in red (significant grouping of 201 high STAI state values), to STAI state coldspots (CS) in blue (significant grouping of 147 low STAI state values), or to the neutral geographic space (NS) in white, for a spatial lag of 600 m. STAI state was adjusted for age, sex, and neighborhood median income. Significance threshold is 0.05 for 999 permutations

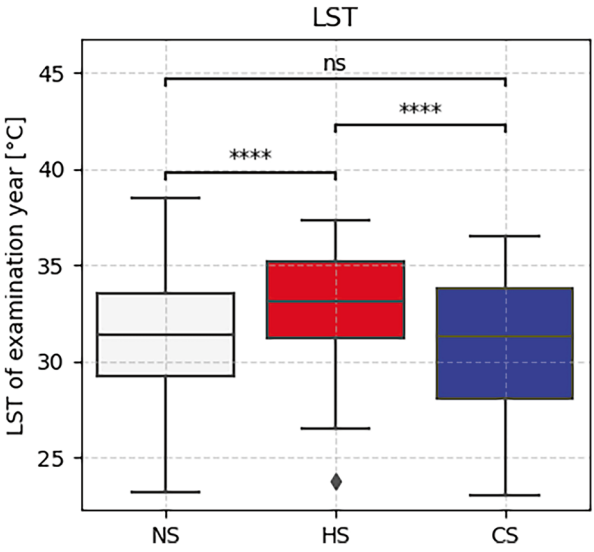

Fig. 4b Boxplots of land surface temperature (LST) values within the three types of State Trait Anxiety Inventory (STAI) state clusters shown on Fig. 4a. High STAI state values show high LST, while low STAI state show low LST. STAI state values where geography's influence is neutral show intermediate LST values. Comparisons (Tukey HSD) between Getis-Ord classes are significant only between hotspots and coldspots and between hotspots and the neutral class. Not significant: $p \geq 0.05$; *: $p \leq 0.05$; **: $p \leq 0.01$; ***: $p \leq 0.001$; ****: $p \leq 0.0001$

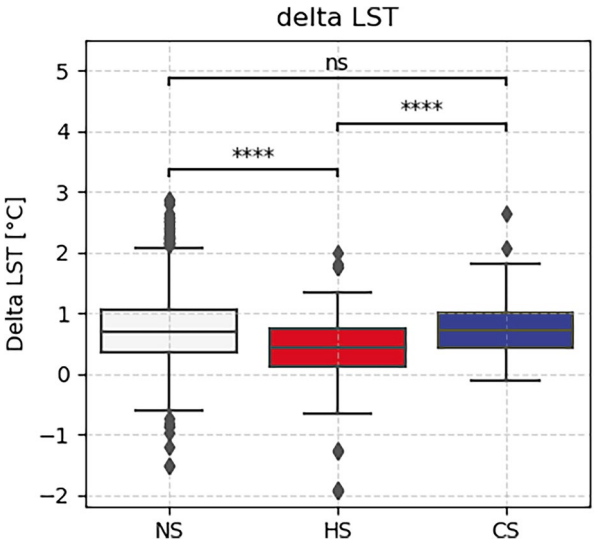

Fig. 4c Boxplots of delta land surface temperature (LST) values within the 3 types of State Trait Anxiety Inventory (STAI) state clusters shown on Fig. 4a. Low STAI state values show low delta LST, while low STAI state show high delta LST. STAI state values where space is neutral show similar delta LST values like in the coldspots. Comparisons (Tukey HSD) between Getis-Ord classes are significant only between hotspots and coldspots and between hotspots and the neutral class. Not significant: $p \geq 0.05$; *: $p \leq 0.05$; **: $p \leq 0.01$; ***: $p \leq 0.001$; ****: $p \leq 0.0001$

Brain's White Matter Microstructure

To represent the strength and significance of the relationships between the four MRI-derived maps (myelin content, axonal density, free water, and tract volume) for the 31 tracts investigated and the LST measurements, we examined the standardized parameter estimates of association, displayed in Fig. 5. LST of the examination year is the explanatory variable in the upper graph, while delta LST is shown in the lower graph.

The myelin content (MT), the axonal density (ICVF), and the tract volume (number of voxels) were not significantly associated with LST. However, we observed a positive correlation between LST and water content (ISOVF) for 20 out of the 31 tracts.

The relationship between delta LST and the tracts revealed only one significant association. Delta LST was weakly but negatively correlated with the number of voxels in the OR left tract. Due to the limited magnitude of this association and to the absence of significance in other parameter estimates, we opted not to conduct further investigation on this specific result.

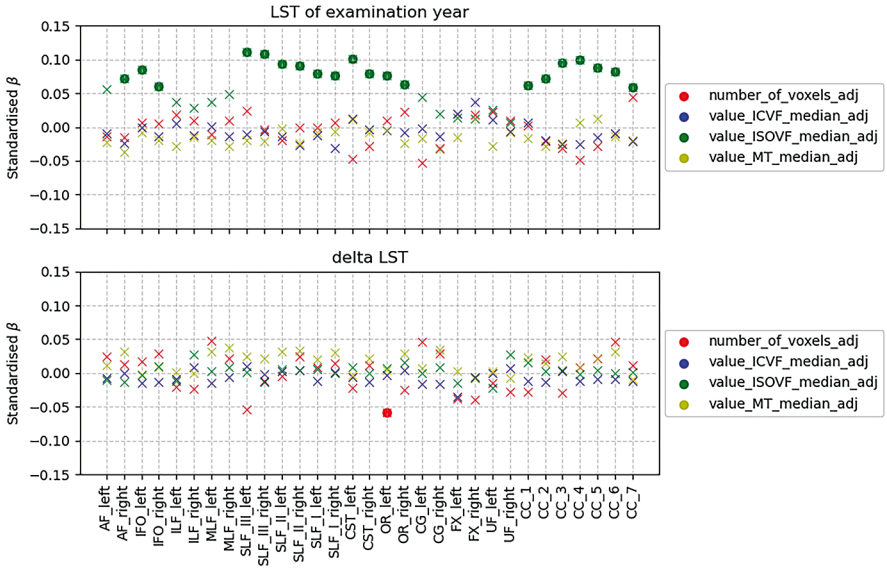

Fig. 5 Relationship between the land surface temperature (LST) (top) and delta LST (bottom) variables and the four MRI-derived maps (myelin content, axonal density, free water, and tract volume) for each of the 31 tracts of interest (on the x-axis). The y-axis shows the standardized parameter estimates. A cross indicates that the parameter estimate for the corresponding map in that tract is not significant, and a dot means that the relationship is significantKey: AF arcuate fasciculus, CG cingulum bundle, CST cortico-spinal tract, FX fornix, IFOF inferior fronto-occipital fasciculus, ILF inferior longitudinal fasciculus, MLF middle longitudinal fasciculus, OR optic radiation, SLF superior longitudinal fasciculus, UF uncinate fasciculus, CC corpus callosum, ICVF intra-cellular volume fraction, ISOVF isotropic volume fraction

The CST left, SLF III left, and CC 4 tracts exhibited the highest significant parameter estimates in the OLS (Fig. 5, top graph). Consequently, we performed a Getis-Ord analysis with a 600 m spatial lag on the free water (ISOVF) value in combination with the LST of the examination year, focused on these selected tracts. By selecting one tract from the association tracts (SLF), the projection tracts (CST), and the corpus callosum (CC), we ensured a representative sample of all tracts of interest.

The obtained three spatial maps show similar spatial patterns. We selected the spatial autocorrelation clusters for free water content in tract SLF III left (largest effect size) to illustrate the results (Fig. 6a). We detected a large coldspot in the northeastern part of the city, whereas hotspots were distributed throughout the remaining urban area.

To assess the differences in variance across Getis-Ord clusters, we conducted a Levene's test, revealing nonhomogeneous variances for the three tracts within the cluster classes. Through the subsequent application of the KW test, we observed effect sizes of 0.023, 0.032, and 0.020 for CST left, SLF III left, and CC 4, respectively. The boxplots in Fig. 6b display the distribution of LST within the spatial clusters of free water content in SLF III left. The primary finding is that LST is significantly higher in hotspots of free water content compared to coldspots. Individuals residing in areas with lower LST equally exhibit lower water content in the CST left and CC 4 tracts.

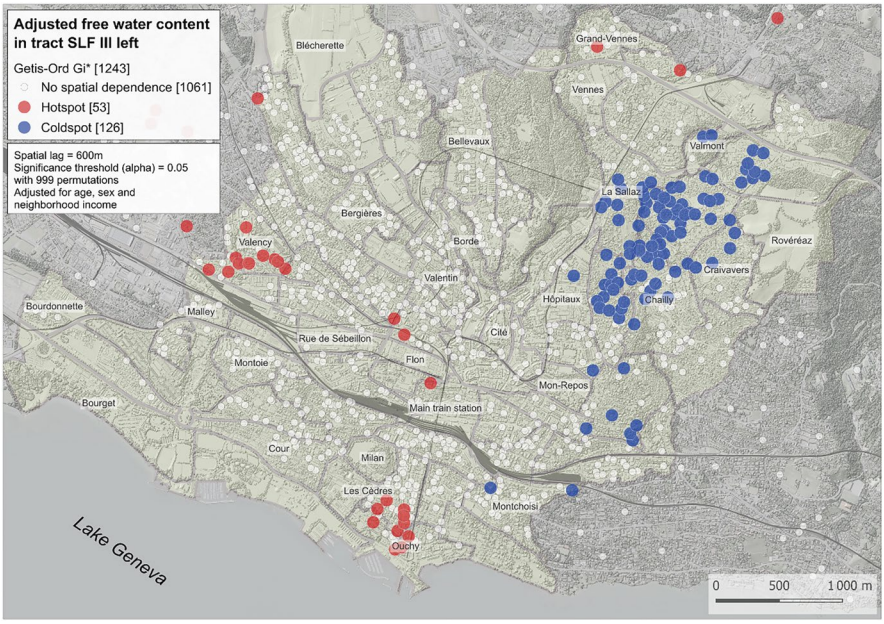

Fig. 6a A dot represents a single subject. Subjects belong either to free water content in tract superior longitudinal fasciculus (SLF) III left hotspots (HS) in red (significant grouping of 53 high water content values), to water content coldspots (CS) in blue (significant grouping of 126 low water content values), or to the neutral geographic space (NS) in white, for a spatial lag of 600 m. Water content in tract SLF III left was adjusted for age, gender, and neighborhood median income. Significance threshold is 0.05 for 999 permutations

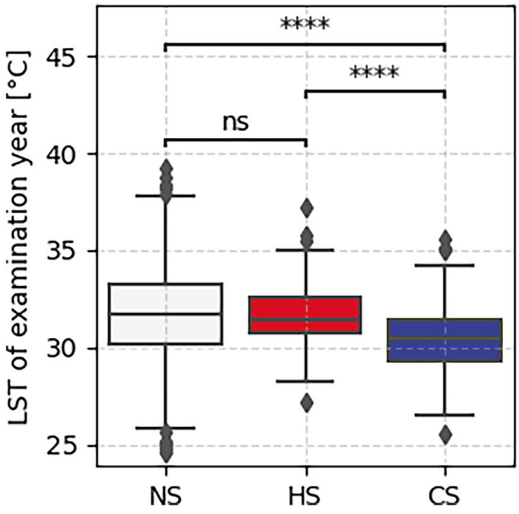

Fig. 6b Boxplots of land surface temperature (LST) values within the three types of clusters of free water content (ISOVF) in tract superior longitudinal fasciculus (SLF) III left shown on Fig. 6a. ISOVF hotspots show higher LST than in coldspots, while their LST mean is not significantly different from the neutral geographic space. Comparisons (Tukey HSD) between Getis-Ord classes are significant only between hotspots and coldspots and between coldspots and the neutral class. Not significant: $p \geq 0.05$; *: $p \leq 0.05$; **: $p \leq 0.01$; ***: $p \leq 0.001$; ****: $p \leq 0.0001$

Discussion

Land Surface Temperature

The geographic distribution of LST values across the urban area of interest (Fig. 1) aligns with our expectations, i.e., densely built-up areas exhibit significantly higher soil temperatures. Conversely, vegetated areas show lower soil temperatures. This is consistent with findings in the existing literature (Gago et al., 2013). However, the average temperature increase over the two periods (delta LST), as illustrated in Fig. 2b, reveals interesting patterns. It was not expected that the city center would experience a lower temperature increase compared to the surrounding areas. This observation highlights the contrasting temperature dynamics between the densely built downtown area where high LST values already existed in 2004, and its more rural surrounding regions. While the urban core maintained consistently high temperatures, the peripheral areas had undergone notable warming over the studied period, mainly because of urban expansion, extensive construction activities of new housings and new industrial zones (Dutta et al. 2019).

Mental Health Variables

We hypothesized that global warming, specifically the occurrence of heat waves in urban areas, may impact well-being and mental health, potentially leading to an increase in mood disorders. The results obtained in fact only partly support this assumption as they point to a temporal distinction affecting the impact of soil temperature on mental health variables. Indeed, both GAF-current coldspots and STAI hotspots, which denote impaired mental functioning and high anxiety, are the areas with the highest LST (see Figs. 3b and 4b). These findings are in concordance with earlier studies that have explored similar relationships (Hansen et al. 2008; Berry et al., 2010).

On the other hand, when we consider the difference (delta) in average LST between the periods 2004–2012 and 2014–2021, it turns out that we observe the opposite phenomenon, i.e., better mental health and moderate anxiety where the delta is the highest (Figs. 3c and 4c). On the contrary, people are worse off where the LST delta is lower (i.e., where the LST has only slightly increased, or even decreased). This finding not only contradicts our initial hypothesis but also previous research (Obradovich et al., 2018). However, this matches specific observations underlined in a systematic review on the impact of climate change on mental health, where Cancioni and colleagues (2020) mention the observation that climate change may have different impacts in different geographical areas, with different timings and with different types of threats to public health. They stress the fact that the effects of climate change can be direct or indirect, and also short-term or long-term. Acute events are likely to act through mechanisms similar to that of traumatic stress, and this is what we observe with the association between punctual high LST and poorer mental health. But we could find no information in the literature regarding a possible mechanism of (mental) adaptation to a gradual increase in delta LST over decades. Finally, to explain why areas with high LST deltas show good mental functioning and low anxiety may be understood as a logical consequence of the results obtained from the LST analysis. As we have observed that areas with high LST already experienced high temperatures 10 years ago, it may be the case that a deterioration in mental health already occurred in the concerned subjects at the end of the previous decade (1995–2004 compared to 2004–2012) and therewith outside the time window of the study.

White Matter Data

The analysis and interpretation of the relationship between WM tracts, mood disorder, and environmental stress like high land surface temperatures in urban areas come within the scope of a largely unexplored field (Amiri et al., 2021). The link between WM tracts and mood disorder is mainly documented by a meta-analysis of 37 different imaging studies of the brain's white matter in patients with depression,

bipolar disorder, and anxiety disorders proposing that these diseases share a common pattern of white matter disruption (Jenkins et al., 2016) and recently confirmed by Parsaei et al. (2024) in their review on WM alterations to be associated with social anxiety disorders.

Our statistical investigations mainly revealed a weak but significant association between LST and water content (ISOVF) in several WM tracts. Spatial autocorrelation analysis showed that spatial clusters of lower ISOVF values were found in areas with lower LST. However, the opposite trend—where higher LST would characterize hotspots of high ISOVF values—was not observed, what would have been consistent with the fact that increased free water is associated with chronic bipolar disorders (Tuozzo et al., 2018), and thus confirming the link observed between mental disorders and high LST. Here the low water content cluster is probably rather due to an older population than in other urban districts of the city. Indeed, this coldspot fits the *Chailly*, *Craivavers*, and *Rovéréaz* districts where 19,6% of inhabitants are 65 years of age and more, while the downtown urban districts like "Centre" typically show 10,7% of inhabitants of the same age class. The brain undergoes structural changes with age, and there may be a gradual decrease in water content in both gray and white matter (Giorgio et al. 2010). This goes along with neurological disorders (multiple sclerosis, leukodystrophies, or other demyelinating disorders) leading to alterations in the brain's WM, including changes in water content (Liu et al. 2017). Anyways, all observations and spatial patterns (Fig. 6a) were consistent for all three brain tracts investigated. The interpretation of these findings, however, requires further investigation.

Limitations and Strengths

While extracting LST from satellite imagery provided valuable insights into surface temperature patterns, it is important to recognize that the perceived air temperature by the local population may differ from the LST values obtained from satellite data. Variables like wind speed, humidity, and local microclimates can impact individuals' perception and experience of temperature, influencing human comfort, well-being and mental health differently across various city areas. Ideally, one should consider complementing LST data with air temperature measurements from local weather stations and potentially include surveys on human thermal comfort for a more accurate representation of the population's experienced temperature.

The current study's analysis of delta LST provides a generalized representation of the average temperature increase over two periods of approximately 10 years. A longer-term longitudinal study would permit a more detailed examination of the impact of specific local temperature changes experienced at each subject's residence. Another limitation of our study arises from the delta LST measurements extending through 2021, to align with brain scans conducted during the third follow-up, while the assessment of mood variables was completed during the second follow-up, concluding in 2017.

Conversely, a significant merit of this study lies in analyzing mental health variables and cerebral tracts in a geographic context, leveraging spatial statistics, and quantifying spatial dependence. The geographical dimension facilitates the integration of environmental and neurological information to better comprehend health challenges associated with the accentuation of the climate warming phenomenon, particularly affecting urban populations.

Conclusion

Employing spatial analysis techniques, we investigated the impact of global warming, specifically focusing on urban heat islands, on mood disorders and WM tracts in the human brain. The study narrowed its scope to urban districts constituting the agglomeration of Lausanne, Switzerland, analyzing data from participants in the CoLaus-PsyColaus study. Positive and statistically significant associations were observed between mood disorders, characterized by the GAF and STAI state and land surface temperature (LST). Higher levels of mental well-being were identified in areas with significantly lower LST, while regions with elevated LST exhibited associations with poorer mental health. The analysis of LST increase revealed a significantly higher delta LST for subjects with better mental health scores, whereas individuals with mood disorders experienced a greater temperature rise (only for the GAF). Additionally, the assessment of various WM tracts in the brain unveiled a significant positive correlation between water content (ISOVF) and LST. Lower water content was linked to lower LST, with no significant evidence found for higher water content in areas with high LST.

References

Amiri, M., Peinkhofer, C., Othman, M. H., Vecchi, T. D., Nersesjan, V., & Kondziella, D. (2021). Global warming and neurological practice: Systematic review. *PeerJ, 9*, e11941. https://doi.org/10.7717/peerj.11941

Anselin, L. (1995). Local indicators of spatial association—LISA. *Geographical Analysis, 27*, 93–115. https://doi.org/10.1111/j.1538-4632.1995.tb00338.x

Bell, C. C. (1994). DSM-IV: Diagnostic and statistical manual of mental disorders. *JAMA, 272*(10), 828–829. https://doi.org/10.1001/jama.1994.03520100096046

Berry, H. L., Bowen, K., & Kjellstrom, T. (2010). Climate change and mental health: A causal pathways framework. *International Journal of Public Health, 55*(2), 123–132. https://doi.org/10.1007/s00038-009-0112-0

Caniani, D., Labella, A., Lioi, D. S., Mancini, I. M., & Masi, S. (2016). Habitat ecological integrity and environmental impact assessment of anthropic activities: A GIS-based fuzzy logic model for sites of high biodiversity conservation interest. *Ecological Indicators, 67*, 238–249. https://doi.org/10.1016/j.ecolind.2016.02.038

Chrisman, N. R. (2020). History of geographic information systems. *International Encyclopedia of Human Geography*, 43–47. https://doi.org/10.1016/b978-0-08-102295-5.10555-4

Cianconi, P., Betrò, S., & Janiri, L. (2020). The impact of climate change on mental health: A systematic descriptive review. *Frontiers in Psychiatry, 11*. https://www.frontiersin.org/journals/psychiatry/articles/10.3389/fpsyt.2020.00074

Coe, R. (2002). *It's the effect size, stupid ! What effect size is and why it is important*. British Educational Research Association annual conference, September 12–14, Exeter, United Kingdom.

Colantonio, A., Moldofsky, B., Escobar, M., Vernich, L., Chipman, M., & McLellan, B. (2011). Using geographical information systems mapping to identify areas presenting high risk for traumatic brain injury. *Emerging Themes in Epidemiology, 8*(1), 7. https://doi.org/10.1186/1742-7622-8-7

Delgado-Saborit, J. M., Guercio, V., Gowers, A. M., Shaddick, G., Fox, N. C., & Love, S. (2021). A critical review of the epidemiological evidence of effects of air pollution on dementia, cognitive function and cognitive decline in adult population. *Science of the Total Environment, 757*, 143734. https://doi.org/10.1016/j.scitotenv.2020.143734

Di Lorenzo, A., Mangone, I., Colangeli, P., Cioci, D., Curini, V., Vincifori, G., Mercante, M. T., Di Pasquale, A., Radomski, N., & Iannetti, S. (2023). One health system supporting surveillance during COVID-19 epidemic in Abruzzo region, southern Italy. *One Health, 16*, 100471. https://doi.org/10.1016/j.onehlt.2022.100471

Dimitrov-Discher, A., Wenzel, J., Kabisch, N., Hemmerling, J., Bunz, M., Schöndorf, J., Walter, H., Veer, I. M., & Adli, M. (2022). Residential green space and air pollution are associated with brain activation in a social-stress paradigm. *Scientific Reports, 12*(1), 10614. https://doi.org/10.1038/s41598-022-14659-z

Duffy, K. A., Green, P. A., & Chartrand, T. L. (2020). Mimicry and modeling of health(-risk) behaviors: How others impact our health(-risk) behaviors without our awareness. *Journal of Nonverbal Behavior, 44*(1), 5–40. https://doi.org/10.1007/s10919-019-00318-x

Dutta, D., Rahman, A., Paul, S. K., & Kundu, A. (2019). Changing pattern of urban landscape and its effect on land surface temperature in and around Delhi. *Environmental Monitoring and Assessment, 191*(9), 551. https://doi.org/10.1007/s10661-019-7645-3

Ermida, S. L., Soares, P., Mantas, V., Göttsche, F.-M., & Trigo, I. F. (2020). Google earth engine open-source code for land surface temperature estimation from the Landsat series. *Remote Sensing, 12*(9), 1471. https://doi.org/10.3390/rs12091471

Firmann, M., Mayor, V., Vidal, P. M., Bochud, M., Pécoud, A., Hayoz, D., Paccaud, F., Preisig, M., Song, K. S., Yuan, X., Danoff, T. M., Stirnadel, H. A., Waterworth, D., Mooser, V., Waeber, G., & Vollenweider, P. (2008). The CoLaus study: A population-based study to investigate the epidemiology and genetic determinants of cardiovascular risk factors and metabolic syndrome. *BMC Cardiovascular Disorders, 8*(1), 6. https://doi.org/10.1186/1471-2261-8-6

Gago, E. J., Roldan, J., Pacheco-Torres, R., & Ordóñez, J. (2013). The city and urban heat islands: A review of strategies to mitigate adverse effects. *Renewable and Sustainable Energy Reviews, 25*, 749–758. https://doi.org/10.1016/j.rser.2013.05.057

Getis, A., & Ord, J. K. (1992). The analysis of spatial association by use of distance statistics. *Geographical Analysis, 24*(3), 189–206. https://doi.org/10.1111/j.1538-4632.1992.tb00261.x

Giorgio, A., Santelli, L., Tomassini, V., Bosnell, R., Smith, S., De Stefano, N., & Johansen-Berg, H. (2010). Age-related changes in grey and white matter structure throughout adulthood. *NeuroImage, 51*(3), 943–951. https://doi.org/10.1016/j.neuroimage.2010.03.004

Goodchild, M. F. (1992). Geographical information science. *International Journal of Geographical Information Systems, 6*(1), 31–45. https://doi.org/10.1080/02693799208901893

Hansen, A., Bi, P., Nitschke, M., Ryan, P., Pisaniello, D., & Tucker, G. (2008). The effect of heat waves on mental health in a temperate Australian City. *Environmental Health Perspectives, 116*(10), 1369–1375. https://doi.org/10.1289/ehp.11339

Hondula, D. M., Balling, R. C., Vanos, J. K., & Georgescu, M. (2015). Rising temperatures, human health, and the role of adaptation. *Current Climate Change Reports, 1*(3), 144–154. https://doi.org/10.1007/s40641-015-0016-4

Jabbar, M., Yusoff, M. M., & Shafie, A. (2022). Assessing the role of urban green spaces for human Well-being: A systematic review. *GeoJournal, 87*(5), 4405–4423. https://doi.org/10.1007/s10708-021-10474-7

Jenkins, L. M., Barba, A., Campbell, M., Lamar, M., Shankman, S. A., Leow, A. D., Ajilore, O., & Langenecker, S. A. (2016). Shared white matter alterations across emotional disorders: A voxel-based meta-analysis of fractional anisotropy. *NeuroImage: Clinical, 12*, 1022–1034. https://doi.org/10.1016/j.nicl.2016.09.001

Julian, L. (2011). Measures of anxiety: State-Trait Anxiety Inventory (STAI), Beck Anxiety Inventory (BAI), and Hospital Anxiety and Depression Scale-Anxiety (HADS-A). *Arthritis Care & Research, 63 Suppl 11*, S467. https://doi.org/10.1002/acr.20561

Kruskal, W. H., & Wallis, W. A. (1952). Use of ranks in one-criterion variance analysis. *Journal of the American Statistical Association, 47*(260), 583–621. https://doi.org/10.1080/01621459.1952.10483441

Kühn, S., Düzel, S., Eibich, P., Krekel, C., Wüstemann, H., Kolbe, J., Martensson, J., Goebel, J., Gallinat, J., Wagner, G. G., & Lindenberger, U. (2017). In search of features that constitute an "enriched environment" in humans: Associations between geographical properties and brain structure. *Scientific Reports, 7*(1), Article 1. https://doi.org/10.1038/s41598-017-12046-7

León, F. R., & Burga-León, A. (2015). How geography influences complex cognitive ability. *Intelligence, 50*, 221–227. https://doi.org/10.1016/j.intell.2015.04.011

Levene, H. (1960). Robust tests for equality of variances. In I. Olkin, H. Hotelling, et al. (Eds.), *Contributions to probability and statistics: Essays in honor of Harold Hotelling* (pp. 278–292). Stanford University Press.

Liu, H., Yang, Y., Xia, Y., Zhu, W., Leak, R. K., Wei, Z., Wang, J., & Hu, X. (2017). Aging of cerebral white matter. *Ageing Research Reviews, 34*, 64–76. https://doi.org/10.1016/j.arr.2016.11.006

Longley, P. (2005). *Geographical information systems: Principles techniques applications and management* (2nd ed.). Wiley.

Louis, S., Carlson, A. K., Suresh, A., Rim, J., Mays, M., Ontaneda, D., & Dhawan, A. (2023). Impacts of Climate Change and Air Pollution on Neurologic Health, Disease, and Practice. *Neurology, 100*(10), 474–483. https://doi.org/10.1212/WNL.0000000000201630

Marteau, T. M., Hollands, G. J., & Fletcher, P. C. (2012). Changing human behavior to prevent disease: The importance of targeting automatic processes. *Science (New York, N.Y.), 337*(6101), 1492–1495. https://doi.org/10.1126/science.1226918

Mathenge, M., Sonneveld, B. G. J. S., & Broerse, J. E. W. (2022). Application of GIS in agriculture in promoting evidence-informed decision making for improving agriculture sustainability: A systematic review. *Sustainability, 14*(16), Article 16. https://doi.org/10.3390/su14169974

MeteoSwiss. (2023). *Urban heat—MeteoSwiss*. https://www.meteoswiss.admin.ch/climate/the-climate-of-switzerland/urban-heat.html

MicroGIS. (2017). *Données Statistiques – Swiss Facts*, https://microgis.ch/prestations/donnees-statistiques/

Moran, P. A. P. (1950). Notes on continuous stochastic phenomena. *Biometrika, 37*(1/2), 17–23. https://doi.org/10.2307/2332142

Obradovich, N., Migliorini, R., Paulus, M. P., & Rahwan, I. (2018). Empirical evidence of mental health risks posed by climate change. *Proceedings of the National Academy of Sciences, 115*(43), 10953–10958. https://doi.org/10.1073/pnas.1801528115

Openshaw, S. (1984). Ecological fallacies and the analysis of areal census data. *Environment and Planning A: Economy and Space, 16*(1), 17–31. https://doi.org/10.1068/a160017

Padhy, S. K., Sarkar, S., Panigrahi, M., & Paul, S. (2015). Mental health effects of climate change. *Indian Journal Of Occupational And Environmental Medicine, 19*(1), 3–7. https://doi.org/10.4103/0019-5278.156997

Palinkas, L. A., & Wong, M. (2020). Global climate change and mental health. *Current Opinion in Psychology, 32*, 12–16. https://doi.org/10.1016/j.copsyc.2019.06.023

Park, Y.-S., McMorris, B. J., Pruinelli, L., Song, Y., Kaas, M. J., & Wyman, J. F. (2021). Use of geographic information systems to explore associations between neighborhood attributes and

mental health outcomes in adults: A systematic review. *International Journal of Environmental Research and Public Health, 18*(16), Article 16. https://doi.org/10.3390/ijerph18168597

Parsaei, M., Hasehmi, S. M., Seyedmirzaei, H., Cattarinussi, G., Sambataro, F., Brambilla, P., & Delvecchio, G. (2024). Microstructural white matter alterations associated with social anxiety disorders: A systematic review. *Journal of Affective Disorders, 350*, 78–88. https://doi.org/10.1016/j.jad.2024.01.118

Pedro, J., Silva, C., & Pinheiro, M. D. (2019). Integrating GIS spatial dimension into BREEAM communities sustainability assessment to support urban planning policies, Lisbon case study. *Land Use Policy, 83*, 424–434. https://doi.org/10.1016/j.landusepol.2019.02.003

Preisig, M., Waeber, G., Vollenweider, P., Bovet, P., Rothen, S., Vandeleur, C., Guex, P., Middleton, L., Waterworth, D., Mooser, V., Tozzi, F., & Muglia, P. (2009). The PsyCoLaus study: Methodology and characteristics of the sample of a population-based survey on psychiatric disorders and their association with genetic and cardiovascular risk factors. *BMC Psychiatry, 9*, 9. https://doi.org/10.1186/1471-244X-9-9

Pykett, J. (2018). Geography and neuroscience: Critical engagements with geography's "neural turn". *Transactions of the Institute of British Geographers, 43*(2), 154–169. https://doi.org/10.1111/tran.12213

Spielberger, C., Gorsuch, R., Lushene, R., Vagg, P., & Jacobs, G. (1983). *Manual for the state-trait anxiety inventory*. Consulting Psychologists Press.

Ståhle, L., & Wold, S. (1989). Analysis of variance (ANOVA). *Chemometrics and Intelligent Laboratory Systems, 6*, 259–272. https://doi.org/10.1016/0169-7439(89)80095-4

Thompson, R., Hornigold, R., Page, L., & Waite, T. (2018). Associations between high ambient temperatures and heat waves with mental health outcomes: A systematic review. *Public Health, 161*, 171–191. https://doi.org/10.1016/j.puhe.2018.06.008

Tobler, W. R. (1970). A computer movie simulating urban growth in the Detroit region. *Economic Geography, 46*, 234–240. https://doi.org/10.2307/143141

Trofimova, O., Latypova, A., DiDomenicantonio, G., Lutti, A., de Lange, A.-M. G., Kliegel, M., Stringhini, S., Marques-Vidal, P., Vaucher, J., Vollenweider, P., Strippoli, M.-P. F., Preisig, M., Kherif, F., & Draganski, B. (2023). Topography of associations between cardiovascular risk factors and myelin loss in the ageing human brain. *Communications Biology, 6*(1), Art. 1. https://doi.org/10.1038/s42003-023-04741-1

Tukey, J. W. (1949). Comparing individual means in the analysis of variance. *Biometrics, 5*(2), 99–114. https://doi.org/10.2307/3001913

Tuozzo, C., Lyall, A. E., Pasternak, O., James, A. C. D., Crow, T. J., & Kubicki, M. (2018). Patients with chronic bipolar disorder exhibit widespread increases in extracellular free water. *Bipolar Disorders, 20*(6), 523–530. https://doi.org/10.1111/bdi.12588

Wicki, A., Parlow, E., & Feigenwinter, C. (2018). Evaluation and modeling of urban Heat Island intensity in Basel, Switzerland. *Climate, 6*(3), Article 3. https://doi.org/10.3390/cli6030055

Yu, H., & Fotheringham, A. S. (2022). A multiscale measure of spatial dependence based on a discrete Fourier transform. *International Journal of Geographical Information Science, 36*(5), 849–872. https://doi.org/10.1080/13658816.2021.2017440

Zoungrana, M., Andrianisa, H. A., Yonaba, R., Mabia, A. G., Thiam, S., & Bonkian, B. (2024). A GIS-based approach for improving urban sanitation planning and services delivery: A case study from Ouagadougou, Burkina Faso. *Habitat International, 143*, 102993. https://doi.org/10.1016/j.habitatint.2023.102993